

Dependence of Atrial Fibrillatory Rate Variations Induced by Head-Up/Down Tilt-Test on Autonomic Action

Chiara Celotto^{1,2}, Carlos Sánchez^{1,2}, Mostafa Abdollahpur³, Frida Sandberg³, Pablo Laguna^{1,2}, Esther Pueyo^{1,2}

¹ Aragon Institute of Engineering Research, University of Zaragoza, IIS Aragón, Zaragoza, Spain

² CIBER in Bioengineering, Biomaterials and Nanomedicine, Zaragoza, Spain

³ University of Lund, Lund, Sweden

Abstract

In atrial fibrillation (AF), autonomic nervous system (ANS) differences among individuals may have a substantial influence on the varying effectiveness of anti-AF treatments. This work aimed to assess the relationship between changes in autonomic balance and in atrial fibrillatory rate (AFR) oscillations ($F_f(t)$) induced by head-up (HUT) and head-down (HDT) tilt test. 22 persistent AF (psAF) patients underwent a tilt test protocol and ECGs were recorded and analyzed to extract $F_f(t)$ and its respiratory modulation (ΔF_f). Electrophysiological simulations of stable reentrant rotors in 2D human atrial psAF tissues were performed. Combinations of different levels of parasympathetic stimulation (PSS) by acetylcholine (ACh) and sympathetic stimulation (SS) by isoproterenol (Iso) were tested. The respiratory-related modulation of ACh was modeled by a cyclic temporal variation of ACh. In the patients, HUT/HDT resulted in an increase/decrease in AFR with respect to baseline (BL). Variations in ΔF_f from HDT/HUT to BL/HDT were significantly positively correlated with the variations in mean $F_f(t)$ (\bar{F}_f). In the simulations, higher Iso and/or $\overline{\text{ACh}}$ led to an increase in \bar{F}_f , while ΔF_f was correlated to the range of ACh variation. HUT/HDT increased/decreased AFR, which could be explained by an increase/reduction in SS. The concomitant variation in ΔF_f could be linked to changes in PSS.

1. Introduction

Autonomic nervous system (ANS) alterations have been suggested to have major influence on atrial fibrillation (AF) initiation and maintenance [1]. The imbalance of sympathetic and parasympathetic activity can play a role both as an AF trigger and in the creation of an AF substrate, which is needed for the perpetuation of AF. Assessing autonomic activity in AF patients could be highly relevant, as inter-patient variability in ANS activity might con-

tribute to explain the large differences in the effectiveness of anti-AF therapies between patients.

Heart rate (HR) variability (HRV) is a commonly employed method to measure autonomic tone during normal sinus rhythm (SR). Respiratory sinus arrhythmia (RSA) is a high frequency HRV phenomenon characterized by the variability in HR that occurs in sync with the respiratory cycle, known to be mediated by the parasympathetic branch of the ANS [2]. Nonetheless, this approach is not suitable for assessing autonomic regulation in cases of AF, in which the rhythm is not dictated by the sinus node.

During AF, the frequency of the f-waves in the ECG (F_f), often referred to as atrial fibrillatory rate (AFR) and measured in cycles per minute, has been employed as a surrogate marker for local refractoriness. Observations from different studies have suggested that variations in autonomic balance can result in F_f oscillations over time ($F_f(t)$). Particularly, controlled respiration has been shown to cause short-term modulation of F_f , leading to cyclic fluctuations that were later suppressed by vagal blockade [3, 4]. Other studies [4–6] have indicated that the magnitude of respiratory f-wave frequency modulation (ΔF_f) could provide additional insights into the parasympathetic modulation of the f-wave frequency, similarly to the observations made for RSA in SR.

The objective of this study was to investigate the relationship between autonomic influences and changes in mean $F_f(t)$ (\bar{F}_f) and in ΔF_f during head-up tilt (HUT) and head-down tilt (HDT). The method developed in [5] was here applied to analyze changes in the respiratory AFR modulation in response to tilt in AF patients. The results from clinical signals were subsequently compared with the results from computational simulations performed using 2D atrial models. Particularly, we evaluated different combinations of sympathetic stimulation (SS) and parasympathetic stimulation (PSS), with the latter modulated as a function of the spatio-temporal release pattern of the parasympathetic neurotransmitter acetylcholine (ACh).

2. Methods

2.1. Clinical recordings

The original research population comprised 40 psAF patients, with a mean age of 64 ± 12 years [7]. During the tilt table examination, 12-lead ECGs were recorded in three distinct phases: five minutes during the supine baseline (BL) position, five minutes during the HDT position (-30°) and five minutes during the HUT position ($+60^\circ$). Additional details are provided in [7]. For this study, records were available for only 29 patients, and out of these 29, only 22 had sufficient quality for our analysis.

2.2. Atrial models

Simulations on 7-by-7 cm sheets of tissues representative of psAF were performed. The electrophysiological activity of human atrial cardiomyocytes was described by the Courtemanche action potential (AP) model [8]. Parasympathetic stimulation effects were described by introducing in the Courtemanche model an ACh-activated potassium current (I_{KACH}), as in [9]. To model sympathetic effects, the activation of the β -adrenergic signaling cascade was considered by using Isoproterenol (Iso), a non-specific β -adrenergic agonist, as described in Gonzalez de la Fuente et al. [10]. This involved incorporating concentration-dependent conductance modulation curves to simulate increases in the maximal conductances of I_{CaL} and I_{Ks} , as well as a decrease in the maximal conductance of I_{to} . Electrical remodeling associated with psAF was accounted for by reducing the maximal conductances of I_{to} , I_{CaL} and I_{Kur} by 50%, 70% and 50%, respectively, and increasing the maximal conductance of I_{K1} by 100% as in [11].

To incorporate psAF-induced structural remodeling, we introduced 20% diffuse fibrosis into the model based on the ranges reported experimentally [12]. Specifically, we randomly selected 20% of the nodes and assigned them the MacCannell fibroblast computational model [13]. The conductivity between fibroblasts was reduced fourfold compared to the coupling between myocytes.

A longitudinal conductivity of 0.003 S/cm and a transverse-to-longitudinal conductivity ratio of 0.5 were considered. This corresponds to a longitudinal conduction velocity of 40.0 cm/s for a planar wave, in agreement with values reported for AF patients in previous studies [9].

2.3. Simulated ACh and Iso release patterns

To model respiratory modulation of ACh concentration, the temporal pattern of ACh release was simulated as cyclically varying following a sinusoidal waveform of frequency equal to 0.125 Hz, as done in a previous study [6].

Mean ACh (\overline{ACh}) equal to 0.05 μM and ΔACh (peak-to-peak) equal to 0.1 and 0.025 μM were tested. All the tested ACh values were within ACh ranges reported in preceding studies (0.0 - 0.1 μM) [9].

The effects of β -adrenergic stimulation were simulated using Iso at spatially and temporally fixed concentrations of 0.0, 0.01 and 1 μM .

2.4. Numerical methods and simulations

Electrical propagation in the atria was described by the monodomain model and solved by means of the finite element method in combination with the operator splitting numerical scheme using the software ELVIRA [14].

To establish steady-state conditions, single cells were paced at a fixed cycle length (CL) of 800 ms for a duration of 16 minutes. The steady-state values of the state variables in the cellular models were then used to initialize the multi-cellular models.

Fourteen stimuli at a CL of 800 ms were applied at the bottom edge of the tissue to pre-excite the model. Subsequently, an S1-S2 cross-stimulation protocol was employed to induce a rotor. The first stimulus (S1) was applied at the bottom edge of the tissue, while the second stimulus (S2) was applied onto a 3.5-by-3.5 cm square at the bottom right corner. Following the delivery of the S1 stimulus, the simulations were run for a duration of 12.5 seconds.

2.5. Frequency characterization of f-waves

From the ECGs, $F_f(t)$ was estimated using a model-based approach, as previously described [4]. \overline{F}_f was computed as the average value over time of $F_f(t)$. An orthogonal subspace projection technique was used to extract respiration-related fluctuations in the f-wave frequency trend [5].

From the simulations, voltage time series were extracted from 169 points uniformly distributed across the tissue. For each of the m -th extracted points, the time instant $t_{m,i}$ correspondent to the i -th beat maximum upstroke velocity was determined and the instantaneous frequency was computed as $1/(t_{m,i+1} - t_{m,i})$, for all beat indices i in the recording. The time series of instantaneous frequencies calculated for each tissue point were subjected to power spectral analysis. Spectral “peak-conditioned” selection was performed as in [15] so that the series whose spectrum was not sufficiently peaked were discarded. $F_f(t)$ was eventually computed as the interpolated and resampled mean of the remaining time series. Finally, \overline{F}_f was computed as the temporal mean, while ΔF_f was proportional to the peak-to-peak amplitude of $F_f(t)$ [4].

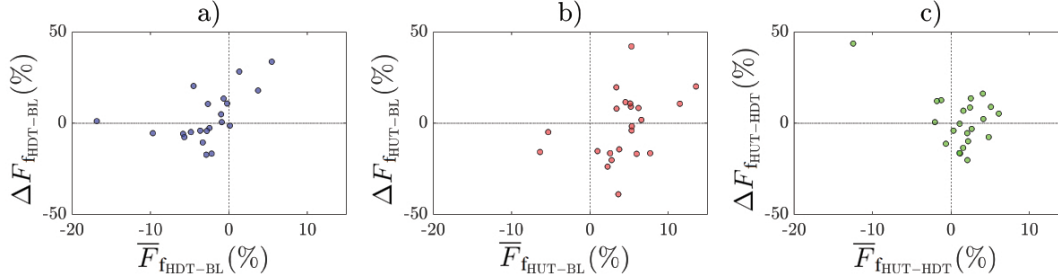


Figure 1. Relative changes in \bar{F}_f vs $\Delta F_f(t)$ measured from patients' ECGs for the three tilt test phases: HDT with respect to BL, HUT with respect to BL and HUT with respect to HDT.

3. Results and Discussion

Examining the relative changes in \bar{F}_f with respect to the relative changes in ΔF_f between the three phases (BL, HDT and HUT), a significant positive correlation was found between the changes, denoted with subscripts referring to the pair of involved stages, $\Delta F_{f_{\text{HDT-BL}}}$ and $\bar{F}_{f_{\text{HDT-BL}}}$ ($\rho=0.58$, $p<0.05$), and between $\Delta F_{f_{\text{HUT-HDT}}}$ and $\bar{F}_{f_{\text{HUT-HDT}}}$ ($\rho=0.41$, $p<0.05$). This is depicted in Figure 1, panels a) and c).

In the simulations, it was observed that an increase in the mean or minimum ACh levels resulted in an increase in \bar{F}_f . Specifically, when ACh remained the same but the minimum value was increased (indicating reduced modulation magnitude as measured by ΔACh), the resulting \bar{F}_f was higher.

The addition of SS by Iso on top of ACh clearly increased the mean frequency in the case of $\Delta\text{ACh}=0.1 \mu\text{M}$. The tested Iso doses (0.01, 1 μM) rendered approximately the same results, with an increase in \bar{F}_f of approximately 0.2 Hz with respect to the case without Iso (Figure 2, panel a). In the cases of the smallest tested ACh variation range ($\Delta\text{ACh}=0.025 \mu\text{M}$), the addition of Iso did not have significant effects on frequency variations (Figure 2, panel b). Finally, ΔF_f was dependent on the range of ACh concentration changes, increasing as the range increased. For the minimum tested variation range of 0.025 μM , the maximum frequency variation was of 0.05 Hz while for the maximum tested ACh variation range of 0.1 μM , the maximum frequency variation was of 0.65 Hz.

A large number of studies have postulated an increase in SS during HUT in SR [16]. In our study, this observation is further reinforced in the context of AF. Specifically, the increase in \bar{F}_f observed in response to the HUT maneuver in AF patients is consistent with the increase in \bar{F}_f that we measured for increased Iso in our simulations, particularly under high ACh. The concurrent variation in ΔF_f also aligns with these findings, as it shows a larger increase in \bar{F}_f coupled with larger increases in ΔF_f in the patients (Figure 1, panel c), which is also reproduced when sim-

ulating increasingly higher Iso concentrations even if to a lower extent in the simulations and only when Iso is varied from 0 to 0.01 or 1 μM .

Although there is scarce research on the autonomic effects during HDT, in SR there is a tendency to associate the slowing of HR during HDT with both an increase in PSS and a decrease in SS [16]. Based on the findings of this work, similar results may not hold true since PSS, causing a shortening of the effective refractory period, actually leads to an increase in \bar{F}_f , as reported in the literature and confirmed by our simulations [17]. Considering the results of our study, the reduction in F_f observed in the psAF patients in response to HDT could be better explained by a reduction in SS, possibly mediated by the cardiopulmonary baroreflex, as indicated by lower F_f in simulated psAF tissues when the Iso concentration was diminished.

Regarding the modulation magnitude, measured by ΔF_f , previous studies have related it to respiratory modulation and parasympathetic activity [4]. In the transitions from BL to HDT and from HDT to HUT, we observed an increase and a decrease in ΔF_f in mean over the psAF population, suggesting an increase and a decrease in PSS, respectively. Taking into account these two transitions and the relationship between relative changes in ΔF_f and \bar{F}_f , it appears that a greater respiratory modulation corresponds to a lesser decline in SS or a greater elevation in SS, respectively. These findings could suggest a potential dependence of SS effects on the underlying level of PSS, as supported by our simulations.

4. Conclusion

The findings of this study suggest that the increase in \bar{F}_f following HUT and the decrease in \bar{F}_f following HDT could be attributed to heightened and diminished sympathetic activity, respectively. PSS, assessed by the magnitude of ΔF_f , appears to exert a modulating role on sympathetic activity rather than being an independent force driving the observed changes in f-wave frequency.

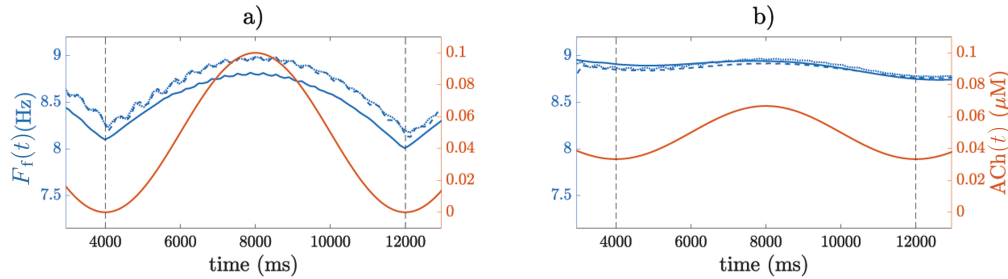


Figure 2. $F_r(t)$ (blue) and $ACh(t)$ (red) from simulations. Solid/dashed/dotted lines represent 0.0/0.01/1 μM Iso.

Acknowledgments

This work was supported by projects PID2019-105674RB-I00, PID2019-104881RB-I00, PID2022-14055 6OB-I00 and TED2021-130459B-I00 funded by MCIN/AEI/10.13039//501100011033 (Spain), ERC G.A. 638284 (ERC), ITN grant 766082 MY-ATRIA (EU) and by European Social Fund (EU) and Gob. Aragón through project LMP94.21 and BSICoS group T39_20R. Computations were performed at the computing facilities of DCMC at Politecnico di Milano.

References

- [1] Chang HY, et al. Effect of Vagotomy on the Activity of Cardiac Autonomic Ganglia: Insight from Left Atrial High Density Frequency Mapping. *International Journal of Cardiology* October 2016;220:435–439. ISSN 01675273.
- [2] Reyes del Paso GA, Godoy J, Vila J. Respiratory sinus arrhythmia as an index of parasympathetic cardiac control during the cardiac defense response. *Biological Psychology* January 1993;35(1):17–35. ISSN 0301-0511.
- [3] Holmqvist F, et al. Rapid Fluctuations in Atrial Fibrillatory Electrophysiology Detected during Controlled Respiration. *American Journal of Physiology Heart and Circulatory Physiology* August 2005;289(2):H754–H760. ISSN 0363-6135, 1522-1539.
- [4] Abdollahpur M, Holmqvist F, Platonov PG, Sandberg F. Respiratory Induced Modulation in f-Wave Characteristics During Atrial Fibrillation. *Frontiers in Physiology* 2021; 12:653492. ISSN 1664-042X.
- [5] Abdollahpur M, Engström G, Platonov PG, Sandberg F. A subspace projection approach to quantify respiratory variations in the f-wave frequency trend. *Frontiers in Physiology* 2022;13. ISSN 1664-042X.
- [6] Celotto C, Sánchez C, Abdollahpur M, Sandberg F, Rodriguez JF, Laguna P, Pueyo E. Effects of Acetylcholine Release Spatial Distribution on the Frequency of Atrial Reentrant Circuits: a Computational Study. volume 49; 1–4.
- [7] Östenson S, Corino VDA, Carlsson J, Platonov PG. Autonomic influence on atrial fibrillatory process: head-up and head-down tilting. *Annals of Noninvasive Electrocardiology The Official Journal of the International Society for Holter and Noninvasive Electrocardiology Inc* March 2017; 22(2). ISSN 1542-474X.
- [8] Courtemanche M, et al. Ionic Mechanisms Underlying Human Atrial Action Potential Properties: Insights from a Mathematical Model. *American Journal of Physiology Heart and Circulatory Physiology* July 1998;275(1):H301–H321. ISSN 0363-6135, 1522-1539.
- [9] Bayer JD, et al. Acetylcholine Delays Atrial Activation to Facilitate Atrial Fibrillation. *Frontiers in Physiology* September 2019;10:1105. ISSN 1664-042X.
- [10] Chronic Atrial Fibrillation Up-Regulates β 1-Adrenoceptors Affecting Repolarizing Currents and Action Potential Duration ;97(2). ISSN 0008-6363.
- [11] Courtemanche M. Ionic Targets for Drug Therapy and Atrial Fibrillation-Induced Electrical Remodeling: Insights from a Mathematical Model. *Cardiovascular Research* May 1999;42(2):477–489. ISSN 00086363.
- [12] Platonov PG, Mitrofanova LB, Orshanskaya V, Ho SY. Structural abnormalities in atrial walls are associated with presence and persistency of atrial fibrillation but not with age. *Journal of the American College of Cardiology* November 2011;58(21):2225–2232. ISSN 1558-3597.
- [13] MacCannell K, et al. A Mathematical Model of Electrotone Interactions between Ventricular Myocytes and Fibroblasts. *Biophysical Journal* June 2007;92(11):4121–4132. ISSN 00063495.
- [14] Heidenreich EA, et al. Adaptive Macro Finite Elements for the Numerical Solution of Monodomain Equations in Cardiac Electrophysiology. *Annals of Biomedical Engineering* 2010;38(7):2331–2345.
- [15] Bailón R, et al. A Robust Method for ECG-Based Estimation of the Respiratory Frequency during Stress Testing. *IEEE transactions on bio medical engineering* July 2006; 53(7):1273–1285. ISSN 0018-9294.
- [16] Gravitational Dose-Response Curves for Acute Cardiovascular Hemodynamics and Autonomic Responses in a Tilt Paradigm ;11. ISSN 2047-9980.
- [17] Cholinergic atrial fibrillation: IK,ACh gradients determine unequal left/right atrial frequencies and rotor dynamics ;59. ISSN 00086363.

Address for correspondence:

Chiara Celotto
 Universidad de Zaragoza, Campus Río Ebro, Edif.I+D, C/ Poeta Mariano Esquillor, s/n, 50018 Zaragoza
 chiaracelotto@unizar.es